Analyst

Accepted Manuscript

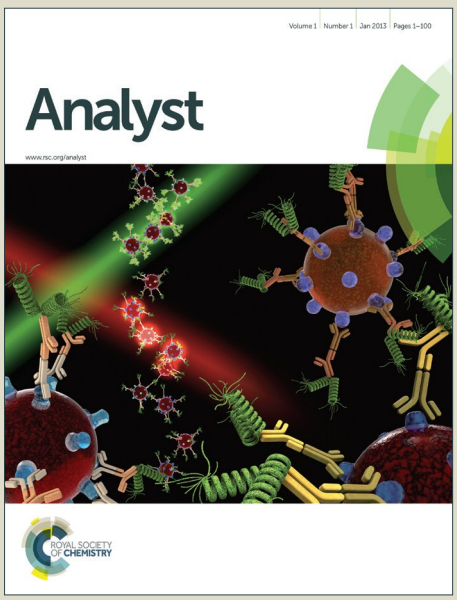

ROYAL SOCIETY OF CHEMISTRY

www.rsc.org/analyst

DEVELOPMENT OF AN INTEGRATED MICROFLUIDIC SOLID-PHASE EXTRACTION AND ELECTROPHORESIS DEVICE

Suresh Kumar, Vishal Sahore, Chad I. Rogers and Adam T. Woolley*

Department of Chemistry and Biochemistry, Brigham Young University, UT 84602-5700, USA

ABSTRACT

This study focuses on the design and fabrication of a microfluidic platform that integrates solid-phase extraction (SPE) and microchip electrophoresis (μCE) on a single device. The integrated chip is a multi-layer structure consisting of polydimethylsiloxane valves with a peristaltic pump, and a porous polymer monolith in a thermoplastic layer. The valves and pump are fabricated using soft lithography to enable pressure-based fluid actuation. A porous polymer monolith column is synthesized in the SPE unit using UV photopolymerization of a mixture consisting of monomer, cross-linker, photoinitiator, and porogens. The hydrophobic, porous structure of the monolith allows protein retention with good through flow. The functionality of the integrated device in terms of pressure-controlled flow, protein retention and elution, on-chip enrichment, and separation is evaluated using ferritin (Fer). Fluorescently labeled Fer is enriched ~80-fold on a reversed-phase monolith from an initial concentration of 100 nM. A five-valve peristaltic pump produces higher flow rates and a narrower Fer elution peak than a three-valve pump operated under similar conditions. Moreover, the preconcentration capability of the SPE unit is demonstrated through μCE of enriched Fer and two model peptides in the integrated system. FA, GGYR, and Fer are concentrated 4-, 12-, and 50-fold, respectively. The loading capacity of the polymer monolith is 56 fmol (25 ng) for Fer. This device lays the foundation for integrated systems that can be used to analyze various disease biomarkers.

*Corresponding author. Phone: 801-422-1701; E-mail address: atw@byu.edu

INTRODUCTION

Analytical techniques are often insensitive to analytes in their crude form.[1-3] Therefore, sample preparation is an essential step in analysis and can involve processes such as dissolution, matrix removal, enrichment, and chemical derivatization.[4] A typical separation analysis may involve >60% of the time in sample preparation, often requiring breakable glassware and solvent volumes ~10X greater than the sample volume.[5-6] Integrating sample preparation with separation techniques on a microfluidic chip can address these problems;[7-8] however, integration can be difficult.[9-10] Solid-phase extraction (SPE) is a common sample preparation method explored for integration in microfluidic systems,[11] with particular emphasis on reversed-phase and affinity SPE.[12-14] A solid SPE support can be built in microfluidic channels by either particle packing or monolith fabrication.[15] Monoliths are gaining popularity because of the ease of on-chip fabrication and ability to tune structure by adjusting the synthesis conditions.[16] Monoliths can be made with alkyl chains such as butyl, octyl (C8), lauryl, or octadecyl (C18) for reverse-phase applications.[17]

The use of on-chip SPE in microfluidics allows enrichment and can improve detection limits.[18-19] Several researchers have integrated SPE and separation techniques in a microfluidic device. Ramsey et al.[19] packed C18-coated silica beads in a microchannel to make an SPE column and integrated it with micellar electrokinetic chromatography separation on a microchip. This integrated device performed an automated sequence of extraction, elution, injection, separation and detection of two model fluorescent dyes in <5 min. Foote et al.[20] used a porous silica membrane to concentrate fluorescently labeled proteins and then separated the enriched proteins by microchip gel electrophoresis. Long et al.[21] used a C18-bead-packed SPE column to enrich rhodamine 123 and fluorescently labeled ephedrine in a polydimethylsiloxane (PDMS)

device. Enriched samples were injected by applying a voltage pulse through a membrane separating the SPE column and separation channel. However, two external syringe pumps were needed for fluid handling, and the SPE column required frits and particle packing. Kang et al.[22] also demonstrated online extraction, electrophoretic separation, and electrochemical detection of dopamine in an integrated multilayer device. A polymeric monolith was fabricated in PDMS, and microvalves were used to control fluid flow. Kaigala et al.[23] developed an integrated microchip platform having monolithic membrane pumps and valves and used it to amplify nucleic acid samples on-chip and then analyze them by microchip electrophoresis. However, these previously reported studies on integration of SPE sample preparation with separation used simple model analytes, required frits to pack particles or had flow driven using external pumps or voltages. In contrast, a truly integrated microfluidic device should perform all sample analysis steps including extraction, enrichment, and separation on a single microchip with on-chip fluid control.

In microfluidic devices, liquids can be manipulated using electrokinetic or pressure-based methods,[24] each of which have merits and demerits. For example, device fabrication is simple and only requires voltage control for electrokinetic operation, but this method is limited by analyte mobility bias, Joule heating, and sensitivity to variations in both fluid composition and channel wall coating.[24-25] On the other hand in pressure-driven systems, a wide range of fluids can be pumped with precise control of volumes, and injection is not biased.[25-26] There are several types of pumps for pressure-driven operation in microfluidics; they involve membranes, electroosmotic flow (EOF), electrohydrodynamics, magnetohydrodynamics or external components.[26] Membrane-actuated peristaltic pumps are of interest as they allow pumping of precise fluid volumes, with easy integration into microfluidic devices. Flow rate and direction

are also easy to control with peristaltic pumps, although they typically require an external solenoid and pressure source for actuation. In this study, a membrane-actuated peristaltic pump and pneumatic valves are used for pressure-based fluid manipulation.

This study focuses on the design and fabrication of an integrated, pressure-driven, reversed-phase SPE and microchip electrophoresis (μCE) system. This work builds on our very recent publication in which we developed and studied a pump and valve injector for μCE, focusing on device fabrication, valve spacing, the injection mechanism, and separation performance.[27] Herein, acrylate-based monoliths with C8 functional groups are used for on-chip capture and enrichment of a protein and peptides. As reverse-phase SPE involves use of organic solvent to elute sample from the solid support, an organic solvent compatible material, cyclic olefin copolymer (COC), is used to make the microchannel that contains the monolith. Furthermore, a multiple-valve peristaltic pump and pneumatic valves are integrated in the system to allow controlled manipulation of fluids. On-chip-extracted samples are eluted from the monolith, injected and then separated in a μCE module. This study demonstrates the integration of sample preconcentration and separation on a single pressure-actuated microchip. This integrated SPE and separation system lays the foundation for the analysis of pre-term birth (PTB) biomarkers and other analytes.

EXPERIMENTAL SECTION

Materials

The integrated device is a four-layer structure consisting of two PDMS and two COC layers. A single-side-polished 100-mm-diameter Si wafer (Desert Silicon, Tempe, AZ) with <100> orientation is used to make fluidic and control layer templates. The PDMS base and

curing agent kit used for fluidic and control layer fabrication is obtained from Dow Chemical (Midland, MI). Tridecafluorooctyltrichlorosilane (UCT, Bristol, PA) is used to prime control and fluidic templates to prevent sticking of cured PDMS to Si. Microfluidic channels for the monolith are enclosed in top and base COC (Zeonor 1020R, Zeon Chemicals, Louisville, KY). Octylmethacrylate (OMA) and Tween 20 are obtained from Scientific Polymer (Ontario, NY) and Mallinckrodt (Paris, KY), respectively. Ethylene glycol dimethacrylate (EGDMA, 98%), 2,2-dimethoxy-2-phenylacetophenone (DMPA, 99%), 1-dodecanol (98%), cyclohexanol, and 2-propanol (IPA) are obtained from Sigma-Aldrich (St. Louis, MO). A SunRay 600 UV lamp (Uvitron International, West Springfield, MA) is used to polymerize monoliths. A biopsy punch (Miltex, York, PA) is used to make 2.5-mm-diameter reservoirs in PDMS layers. Blunt-end, 1.5”-long, 22-gauge needles are obtained from Jansen Global (Santa Barbara, CA) to punch holes in the control PDMS layer. Circuit board drill bits (200- and 550-µm diameter) are purchased from MSC Industrial Supply (Melville, NY) to make holes in top COC plates.

Food dyes (Great Value, Walmart, Bentonville, AR) are filled into microfluidic channels for visual inspection of device operation. Solenoid valves (Clippard, Cincinnati, OH) connected to the building compressed air supply (30 psi) are used to actuate on-chip valves and pumps. The control channel and solenoid are connected using microbore polytetrafluoroethylene (PTFE) tubing (0.022” ID x 0.042” OD, Cole Parmer, Vernon Hills, IL) and hypodermic stainless steel pins (0.025” OD x 0.018” ID x 0.394" length, Type 304, New England Small Tube, Litchfield, NH). Hydroxypropylcellulose (HPC), phenylalanine-alanine (FA), and glycine-glycine-tyrosine-arginine (GGYR) are obtained from Sigma-Aldrich. Ferritin (Fer) is purchased from EMD Millipore (Billerica, MA). Fluorescein isothiocyanate (FITC) and Alexa Fluor 488 5-tetrafluorophenyl ester (ALF) obtained from Life Technologies (Carlsbad, CA) are used to

fluorescently label samples. FA and GGYR are labeled as follows: sodium bicarbonate buffer (BCB, 100 mM) is prepared by dissolving 420 mg $NaHCO_3$ (EMD Chemical, Gibbstown, NJ) in 50 mL of deionized (DI) water, and the pH is adjusted to 9.1 using 6 M NaOH (Spectrum, Gardena, CA), as recommended for overnight labeling. FA and GGYR solutions are prepared in BCB, each containing 10 mM peptide and 1.6 mM FITC. Peptide and FITC mixtures are incubated overnight at room temperature for labeling. Fer labeling involves mixing of 20 µL of a 10 mM solution of FITC in dimethyl sulfoxide (DMSO, Sigma-Aldrich) with 250 µL of 6.7 µM Fer in 100 mM BCB, pH 9. Then, the mixture is incubated in the dark for 24 h at room temperature for labeling. Next, excess dye is removed from the Fer solution using centrifugal membrane filters (EMD Millipore) with mass cutoffs of 30 kDa. Finally, the stock concentration of FITC-Fer is measured using a spectrophotometer (Nanodrop ND-1000, Wilmington, DE). Solid-phase elution solutions are prepared containing 30, 50, 70, and 90% v/v acetonitrile (ACN, Sigma-Aldrich) in 10 mM BCB, or pure (100%) ACN. Electrophoretic separations are performed in 20 mM BCB (pH 9.8), 30 mM NaCl with 0.05% HPC.

Device design

The integrated device has a multi-layer structure, made up of elastomeric and thermoplastic materials. A multi-valve peristaltic pump and a set of four pneumatic valves are incorporated around a ‘T’-shape channel network to manipulate fluids using pressure (see Figure 1A). A 2-mm-long and 25-µm-deep COC channel contains a C8 monolith for reverse-phase SPE. Through holes connect the COC channel to 18-µm-deep fluidic channels in the PDMS layer. Pneumatic valves are 250-µm wide and 22-µm deep, and when placed in groups of 3 or 5 with a 120-µm gap between each valve, they form a peristaltic pump. A fixed valve spacing of 300 µm from the injection intersection to each valve is used. A recently published study indicates that a

200-µm valve spacing provides slightly greater peak heights but similar resolution to a 300-µm valve spacing.[27] Solution flow rate can be controlled using pump actuation frequency, and a simple "T" intersection is used in all devices.

Device fabrication

Each layer of the integrated device is fabricated separately. Fluidic and control Si templates are made using conventional UV photolithography. Si wafers (100-mm diameter) cleaned in buffered oxide etchant (BOE, Transene, Danvers, MA) for 30 s and baked at 150 ºC for 15 min are used to make templates. Cleaned Si wafers are exposed to hexamethyldisilazane (HMDS) vapor at 65 ºC for 5 min to prime the surface. Then, photoresist (AZ 50XT, AZ Electronic Materials, Branchburg, NJ) is spin coated for 65 s on the fluidic and control wafers at 4000 and 1750 rpm to make 13.5- and 22-µm thick photoresist layers, respectively. Photoresist-coated wafers are soft baked at 60 ºC for 10 min to degas the photoresist layer and subsequently at 125 ºC for 3 min. Baked control and fluidic wafers are air cooled for 2 min and placed in a box to rehydrate the photoresist for 40 min to prevent cracking. Then, the fluidic and control wafers are exposed to UV light through a clear-field Cr mask in a UV aligner (Karl Suss America, Waterbury, VT) to transfer mask features into the photoresist layer. Exposed wafers are developed in AZ 400K (AZ Electronics, Somerville, NJ) diluted 1:1 in water for 3-4 min to form fluidic and control channel features. The developed fluidic wafer is heated at 125 ºC for 10 min to reflow photoresist and form rounded features. A post development bake increases the fluidic channel height to ~18 µm. Finally, the fluidic and control layer feature heights are confirmed using an Alpha Step 200 Profilometer (Tencor, Mountain View, CA).

Fluidic and control template features are transferred into PDMS by soft lithography as shown in Figures 1B-C. PDMS base and curing agent are mixed at 4.4:1 and 19:1 ratios for the

control and fluidic layers, respectively, and degassed for 30 min in vacuum. Fluidic and control templates are silanized by exposing to tridecafluorooctyltrichlorosilane vapor at 80 ºC for 10 min. A 4"-diameter PVC ring has its edges coated with degassed control layer PDMS mixture, and the silanized control template is placed on it to make an airtight seal. The PVC ring prevents PDMS leakage and maintains constant material height during polymerization. The assembly is baked on a hot plate at 80 ºC for 10 min to polymerize PDMS. Next, control layer PDMS mixture is poured in the center of the control template and allowed to spread uniformly to cover the features. The silanized fluidic template is spin coated with fluidic layer PDMS mixture to form a uniform coating of 25-28 μm thickness. Finally, the fluidic and control layer PDMS is cured in an oven at 80 ºC for 1 hour. Cured control layer PDMS is peeled off from the template and diced into individual devices, and then holes are punched using a 22-gauge blunt end needle to connect control channels to pressure tubing. Hole-punched control layer PDMS is cleaned using IPA, stamped with curing agent coated on a Si wafer, and aligned and contacted to the fluidic PDMS layer while observing in a modified stereomicroscope. Aligned PDMS layers are baked at 80 ºC for 1 hour to form a bond. Then, the bonded PDMS layers are peeled off from the fluidic template, and reservoir holes are made using a biopsy punch.

In parallel, the COC channels are made using hot embossing and thermal bonding as shown in Figure 1D-E. A 100-mm-diameter oxidized Si template is prepared using standard photolithography to make COC channels; the template is wet etched in 40% aqueous KOH solution at 70 ºC to yield ~25 μm tall features. A 1-mm-thick, 15 x 15 cm^2 COC plate is cut into 3.5 x 2.5 cm^2 pieces using a bandsaw, and edges are smoothed with a razor. Etched Si template features are then hot embossed in the COC at 138 ºC for 26 min. To make the top COC plate, 1-mm-thick COC is cut into 1 x 1 cm^2 pieces using a bandsaw. Each 1-mm-thick COC piece is

thinned to 80-100 μm using a hydraulic press (Carver, Wabash, IN) with top and base platen heated to 196 ºC and ~2 metric tons applied. This thinned COC is again cut into sizes matching the base COC plate, and holes are drilled using a 200-μm-diameter circuit board drill bit. The top COC plate is flattened between two glass slides at 110 ºC for 25 min and thermally bonded to the imprinted base COC at 110 ºC for 28 min. Then, the bonded COC device edges are sealed using cyclohexane, and a C8 monolith is polymerized in the COC channel as described below.

SPE is performed on a solid porous support formed inside a COC channel by in-situ UV photopolymerization of monomer, porogens and crosslinker mixture. A schematic showing monolith fabrication in a COC channel is shown in Figure S1A in the Electronic Supplementary Information (ESI). Monolith solution containing OMA (23%), EGDMA (11%), cyclohexanol (25%), 1-dodecanol (23%), and Tween 20 (17%) and having a total mass of 1.18 g is prepared by weighing in a 10 mL glass vial. The mixture is vortexed for 30 s and sonicated for 5 min. Next, 12 mg of DMPA (1% w/w) is weighed and added to the monolith mixture, followed by vortexing and sonication for 10 min. After that, the mixture is purged with N_2 for 5 min to remove dissolved gas. The COC channel is rinsed with IPA and vacuum dried followed by the introduction of degassed monolith mixture using a 2-μL pipette. The solution flows through the COC channel due to capillary action, and excess solution is removed from the inlet reservoir. A Cr mask with multiple openings is used to cover the solution-filled COC channel, exposing the desired channel area where the solution is polymerized. The assembly is stabilized using electrical tape, a COC spacer of similar thickness is attached to the mask to maintain uniform height, and everything is placed under a SunRay 600 UV floodlight chamber at a 14” distance from the bulb. The UV lamp is turned on at 50 mW/cm^2, and the device is exposed for 11 min. Then, the Cr mask is removed from the device, reservoirs are rinsed with IPA, and

unpolymerized monolith solution is removed by vacuum. The monolith is further rinsed with IPA to remove any unpolymerized components left on the surface, followed by water rinsing to remove IPA. A photograph of a polymerized monolith in a COC device is shown in Figure S1B in the ESI.

The morphology of a bulk-polymerized C8 monolith is observed using a Philips XL30 FEG environmental scanning electron microscope (ESEM) from FEI (Hillsboro, OR). Sample preparation includes polymerization of 200 µL of monolith solution in a polypropylene tube under similar UV exposure. The polymerized monolith is broken into small pieces and mixed in IPA on a shaker overnight to remove unpolymerized solution. Finally, the monolith is stored in vacuum overnight. The dried monolith is placed on a carbon taped stub and examined under ESEM for internal structural information as shown in Figure S1C in the ESI. ESEM imaging shows that fused structures are formed with varying pore sizes, which allow liquid to flow through the monolith structure.

Finally, the PDMS and COC layers are assembled and bonded together as shown in Figure 1E. Briefly, COC and PDMS are cleaned with IPA, dried using a N_2 gun and baked at 80 ºC for 15 min. The COC device surface is further cleaned in an O_2 plasma (Planar Etch II, Technics, Osaka, Japan) for 4 min at 200 W, and the PDMS is stamped in curing agent coated on a wafer. Finally, COC and PDMS are aligned and thermally bonded at 80 ºC for 1.5 h. A photograph of a completed integrated device is shown in Figure 1F.

Device operation overview

In the integrated device (Fig. 1A), labeled analyte is captured and concentrated on the C8 monolith. Sample retained in this SPE unit is next released and then captured at the injection

intersection using valves, and the captured plug is separated by μCE. Reservoir 1 is used to introduce sample, buffer, and ACN mixtures. All solutions except 90% ACN are added to or removed from reservoir 1 as needed using a 10 μL pipette without stopping pump operation. To load 90% ACN in the reservoir, pump actuation is stopped, the prior solution is removed, the reservoir is rinsed with 90% ACN, and then the reservoir is filled with 90% ACN. Reservoirs 2 and 4 collect sample and separation waste, respectively. Reservoirs 3 and 4 are filled with separation buffer and used to apply voltage along the separation channel during μCE.

Device characterization

Devices are initially tested using food dye solutions prepared in 10 mM BCB and 85% ACN. Device design and operational aspects such as pneumatic valve actuation pressure, pump flow rate, dead volume, flow through monolith and sample plug capture are studied. Figures 2A-B show a schematic of an open and closed valve for fluidic and control channels separated with a 6-8 μm thick flexible membrane. Several fluidic channel heights (7-18 μm) are tested for a 65-μm-wide fluidic channel, and 25-50 psi are applied in the control channel to completely close pneumatic valves.

The SPE module is integrated with the separation module to allow on-chip extraction, enrichment and separation. Three- and five-valve peristaltic pumps are fabricated on chip using 250-μm-wide control channels, spaced at a 120-μm distance. Figures 2C-D show photographs of a five-valve peristaltic pump with all valves either open or closed. Figures 2E-F similarly display open and closed configurations of a set of four pneumatic valves placed around the injection intersection with a 300 μm distance from the intersection, for capture of sample plugs prepared in the SPE module. Figure 2G shows a photograph of a microdevice fully set up for integrated operation. The green dye filled tubing connects control reservoirs with external solenoids that

actuate valves. Solenoid operation is controlled using a computer program written in LabVIEW. Three- and five-valve pump flow rates are calculated by recording the time to pump different solutions from the intersection to the sample waste reservoir (4 mm). Pumps are actuated at 10, 20 or 40 Hz with ~30 psi applied.

Protein retention and elution

FITC-Fer is used to study retention and elution on a C8 monolith in the SPE module. A three-valve peristaltic pump is operated at 40 Hz, and valves are actuated with ~30 psi. The C8 monolith surface is conditioned by flowing 90, 50 and 30% ACN solutions for 5 min each, followed by a 5 min 10 mM BCB (pH 9.8) rinse. FITC-labeled Fer (500 nM) is loaded onto the monolith for 5 min, and the column is rinsed by flowing BCB for 5 min. The captured Fer is eluted using increasing amounts of ACN (30, 50, 90 and 100%); elution times were 5 min for all solutions except for 100% ACN, which was flowed for 10 min. Under illumination from a 488 nm laser, monolith images are recorded at each step using a Photometrics CoolSNAP HQ2 (Tucson, AZ) cooled CCD camera with a 500 ms exposure time. To quantify fluorescence, average values are measured by drawing a box (approx. 110 x 400 pixel^2) around the monolith in the fluorescence image using NIH ImageJ software. Protein retention and elution experiments are repeated 2-3 times on different devices with minor modifications in experimental conditions (i.e., column composition, flow rate, and rinse time) to optimize results. Comparable data are obtained in the repeated studies, indicating experimental reproducibility.

The effect of three- vs. five-valve pumps on Fer retention and elution in an integrated device is also studied. After column conditioning, 700 nL of 200 nM FITC-Fer are loaded onto a C8 monolith using a five-valve peristaltic pump operated at 10 Hz, and ~30 psi applied pressure for 5 min. The C8 column is rinsed with BCB, and the captured protein is eluted by flowing 90%

ACN. Content eluted from the column is detected using a photomultiplier tube (PMT; Hamamatsu, Bridgewater, NJ) monitoring fluorescence at the injection intersection. A similar experiment is performed using a three-valve pump operated at 20 Hz and ~30 psi for 15 min. After conditioning, 450 nL of 100 nM FITC-Fer are loaded onto the column, and the captured Fer is eluted in 90% ACN.

Analyte enrichment

An integrated device with a three-valve peristaltic pump is used for FITC-Fer enrichment studies on a C8 monolith. The peristaltic pump is operated at 20 Hz, and the valves are actuated at ~30 psi. After column conditioning, FITC-Fer (100 nM) is loaded for 10 min (~300 nL) and monolith fluorescence images are recorded every minute. Next, the column is washed with 10 mM BCB for 4 min; then, enriched FITC-Fer is eluted using 90% ACN and captured at the injection intersection using the valves. The captured plug is separated with 700 V applied down the separation column, and the fluorescence is recorded with a PMT at a 3-mm distance down the separation column from the injection intersection. Electrophoretic separation of 100 nM FITC-Fer is also performed under similar conditions using a device lacking the C8 monolith.

Enrichment of model peptides (FA and GGYR) on a C8 column is also studied in an integrated device. A three-valve peristaltic pump is operated at 20 Hz, and ~30 psi is used for actuating the valves and pump. Fluorescently labeled FA and GGYR (500 nM each) are loaded onto a preconditioned C8 monolith for 10 min and rinsed with 10 mM phosphate buffer (pH 7.2). The enriched peptides are eluted in 90% ACN and captured using the valves at the intersection. The captured plug is separated into FA and GGYR bands with 700 V applied along the separation column, with PMT fluorescence detection 4 mm from the injection intersection. The

same peptide mixture is similarly separated in a device lacking a C8 monolith. All electrophoretic separations are performed three times in replicate in the same device.

RESULTS AND DISCUSSION

Preliminary experiments on device design were performed to assess PDMS compatibility with ACN, optimize channel dimensions, measure pump flow rates, and observe flow through a monolith. The peristaltic pump was used to pump 85% ACN (used in previous on-chip SPE studies)[28] for 8 hr to observe effects on the cured PDMS. The PDMS did not swell over this time, the pump was still operational after 8 hr of actuation, and no PDMS delamination was observed, all supporting that PDMS is compatible with ACN. Although higher ACN content solvents were used subsequently to improve elution, no negative effects or PDMS incompatibility issues were observed.

Our device configuration (Fig. 1) allowed valve actuation at 30 psi; flow data for three- and five-valve pumps are presented in Table 1. Our valves used a higher actuation pressure than other publications (5 psi)[29] because our channels were narrower and deeper. The five-valve peristaltic pump produced a higher flow rate than the three-valve pump. However, the primary focus of this work was not to compare the two types of pumps in detail. Three-valve pumps were used in initial device designs that generated some of the data in this work; they provided adequate flow for retention/elution studies. Five-valve pumps were designed subsequently to provide higher flow rates and reduce dispersion in eluting retained analyte into the μCE injector in integrated devices. For the five-valve pump, the flow rate increased on increasing the pump actuation frequency. The flow rate for the five-valve pump with 10 Hz actuation was independent of solution composition; however, the flow rates for both types of pumps with 20 Hz actuation increased with acetonitrile content. The composition-dependent flow rates at 20 Hz

may be due to solution viscosity differences, which could affect the extent of valve membrane displacement at the higher actuation rate. However, at the slower (10 Hz) actuation rate, the independence of the flow velocity on solution viscosity may indicate that the valves in the pump close completely with each activation stroke, displacing the full solution volume. The use of thinned (~100-µm-thick) COC and narrow (200-µm-diameter) through holes reduced the dead volume for connecting monolithic columns in COC with PDMS fluid handling, allowing the COC microfluidics to be flushed in <2 min in five-valve pump designs.

In Figure 3 background-subtracted fluorescence intensities of FITC-Fer on a C8 monolith are plotted as a function of retention/elution conditions. The monolith fluorescence intensity increased as the FITC-Fer loading time was raised from 3 to 5 min, due to delivery of more analyte to the column. Rinses of buffer, 30% ACN, and 50% ACN had little effect on column fluorescence because FITC-Fer was strongly retained. However, the column fluorescence decreased significantly when the monolith was rinsed with 90 or 100% ACN, because the high organic content reduced non-polar interactions between FITC-Fer and the C8 monolith, which released the retained protein. Elution with 90% ACN was independent of previous ACN rinses, as 30 or 50% ACN had little effect on protein retention (Fig. 3); we studied 30 and 50% ACN because we previously used these to wash unreacted dye from monoliths in on-chip labeling.[28]

FITC-Fer was loaded onto a C8 monolith using three- and five-valve peristaltic pumps in integrated devices to study the effects of pump type on elution. Fluorescence images of the C8 monolith at different stages of the process using a five-valve pump are shown in Figures 4A-C. Loading of the FITC-Fer on the C8 monolith increased fluorescence signal, while elution of the retained Fer from the monolith in 90% ACN lowered the monolith fluorescence. Even though ~3-fold more FITC-Fer was loaded on the monolith with the five-valve pump compared to the

three-valve pump, elution in 90% ACN using a five-valve peristaltic pump (blue trace in Figure 4D) resulted in a narrower peak than with a three-valve pump (red trace in Figure 4D). Additionally, the larger flow rate of the five-valve pump yielded a faster elution time compared with the three-valve pump. The difference in the peak heights of the eluted Fer bands was largely due to loading of different amounts of Fer on the monolith. The faster flow rate produced by the five-valve pump compared to the three-valve pump (Table 1) reduced the time for diffusion, and hence, longitudinal dispersion of the FITC-Fer band, which resulted in a narrower peak for the five-valve pump. Narrower peaks should allow capture of a larger fraction of eluted analyte at the intersection, resulting in more efficient transfer to the μCE module.

The enrichment capability of the SPE module was evaluated using FITC-Fer. Fluorescent images on a C8 monolith were recorded under different FITC-Fer loading/elution conditions (Figures 5A-F). Fluorescence became brighter as the loading time increased, approaching an asymptotic maximum. For quantitative comparison, the monolith fluorescence was calculated from these images. Fluorescence increased approximately linearly with time for the first 4 min, gradually approached an asymptote by ~8 min, and after 8 min the fluorescence plateaued. The linear increase in fluorescence intensity with time for the first 4 min resulted from complete retention of the loaded FITC-Fer on the monolith. As the loading capacity of the column was approached (5-8 min) the increases in column fluorescence became more gradual with additional loading time. From 8-10 min, the column loading capacity had been reached, so additional retention (or signal increase) was limited. A buffer rinse had almost no effect on monolith fluorescence because FITC-Fer was strongly retained on the C8 column under those conditions. However, monolith fluorescence decreased significantly due to elution when the monolith was

rinsed with 90% or 100% ACN. Similar results were obtained in another experiment carried out under slightly different conditions, confirming reproducibility.

We also quantified FITC-Fer enrichment on the C8 monolith using fluorescence intensity measurements. The fluorescence of 100 nM FITC-Fer in a channel of the same dimensions but lacking a monolith was measured; the FITC-Fer fluorescence on the monolith after the buffer rinse step was 80-fold higher than that in the channel lacking a monolith. This 80-fold sample enrichment should help in improving detection limits for subsequent μCE separation. Additionally, the loading capacity of the monolith was calculated using the linear region (0-4 min) of the plot in Figure 5G. After 4 min, 550 nL of FITC-Fer had been flowed through the monolith, leading to an estimated monolith loading capacity of 56 fmol (25 ng) for Fer. If needed the loading capacity could be increased by making longer monoliths, creating monoliths with greater surface area, or forming several monoliths in parallel channels. Notably, FITC-Fer elution occurred effectively in 90% ACN flowed directly after buffer rinses.

We further combined this on-chip enrichment and elution with μCE in an integrated device. Labeled analyte was loaded/enriched on the monolith, eluted with 90% ACN into the injection intersection, and then the captured plug was separated by μCE. Figure 6A shows separation of FITC-Fer after on-chip enrichment, while Figure 6B shows a FITC-Fer separation for the same loaded concentration (100 nM) without enrichment. The FITC-Fer peak height in μCE increased 50-fold with enrichment, close to the 80-fold concentration gain determined from monolith fluorescence. The presence of ACN in the enriched FITC-Fer plug in Figure 6A also decreased the migration time relative to that in Figure 6B. A mixture of fluorescently labeled FA and GGYR was also loaded and enriched on a C8 monolith, eluted into the injector, and separated by μCE similar to FITC-Fer. Figure 6C shows separation of labeled FA and GGYR

after on-chip enrichment; Figure 6D shows separation of the same analytes at the same concentration (500 nM) without enrichment. The FA and GGYR peaks increased approximately 4- and 12-fold after enrichment, respectively. Because FA and GGYR are less hydrophobic than Fer, they are less retained on the monolith, resulting in lower enrichment factors than for Fer. Overall, this integrated device shows promising results for on-chip peptide and protein enrichment for electrophoretic separation.

CONCLUSIONS

A fabrication process was developed to make integrated multilayer solid-phase extraction and electrophoresis microdevices. On-chip pneumatic valves and a peristaltic pump were formed in an elastomeric material to enable pressure-actuated fluid manipulation. In the integrated design, the thermoplastic layer thickness and hole diameter were reduced to decrease dead volume. Fluidic and control channel dimensions were optimized to actuate valves with 30 psi and produce reasonable flow rates. Both three- and five-valve pumps were evaluated; higher flow rates and narrower elution profiles were obtained with five-valve pumps. FITC-Fer was enriched 80-fold on a C8 monolith in an integrated device, resulting in a 50-fold increase in μCE peak height. On the other hand, peptides were enriched 4-12 fold, due to their lower retention than Fer on our monolith. Overall, this study lays the foundation for devices integrating SPE, elution and μCE for preterm birth biomarker analysis.

In the future, multiple valved inlet channels can be included in the device design to avoid repeated reservoir rinse and solution replacement steps that are needed with the current device design. Furthermore, this work could be extended to include on-chip fluorescent labeling,[28] which is often a time-consuming off-chip sample preparation step. Additionally, an affinity monolith could be incorporated in a modified device to allow selective capture of target analytes

in the system.[30] Such integration of affinity extraction, SPE, fluorescent labeling, and μCE on a single platform could offer a rapid, sensitive, and potentially inexpensive platform for PTB biomarker analysis or for other biomedical analyte determinations.

ACKNOWLEDGEMENTS

We are grateful to the National Institutes of Health (R01 EB006124) for support of this work. We are also thankful to Dr. Radim Knob for providing an SEM image of a C8 monolith.

REFERENCES

1. E. Carasek and J. Merib, *Anal. Chim. Acta*, 2015, **880**, 8-25.
2. L. M. L. Nollet and F. Toldra, *Handbook of Food Analysis*, CRC Press, 3rd edn., **2015**.
3. G. Vas and K. Vékey, *J. Mass Spectrom.*, 2004, **39**, 233-254.
4. J. Pawliszyn, *Anal. Chem.*, 2003, **75**, 2543-2558.
5. S. Ulrich, *J. Chromatogr. A*, 2000, **902**, 167-194.
6. L. Nováková and H. Vlčková, *Anal. Chim. Acta*, 2009, **656**, 8-35.
7. B. M. Paegel, R. G. Blazej and R. A. Mathies, *Curr. Opin. Biotechnol.*, 2003, **14**, 42-50.
8. G. M. Whitesides, *Nature*, 2006, **442**, 368-373.
9. T. Thorsen, S. J. Maerkl and S. R. Quake, *Science*, 2002, **298**, 580-584.
10. P. N. Nge, C. I. Rogers and A. T. Woolley, *Chem. Rev.*, 2013, **113**, 2550-2583.
11. J. Kim, M. Johnson, P. Hill and B. K. Gale, *Integr. Biol.*, 2009, **1**, 574-586.
12. P. N. Nge, J. V. Pagaduan, M. Yu and A. T. Woolley, *J. Chromatogr. A*, 2012, **1261**, 129-135.
13. X. Sun, W. Yang, T. Pan and A. T. Woolley, *Anal. Chem.*, 2008, **80**, 5126-5130.
14. A. Żwir-Ferenc and M. Biziuk, *Pol. J. Environ. Stud.*, 2006, **15**, 677-690.

15. J. P. Kutter, *J. Chromatogr. A*, 2012, **1221**, 72-82.

16. F. Svec and Y. Lv, *Anal. Chem.*, 2014, **87**, 250-273.

17. K. Liu, P. Aggarwal, J. S. Lawson, H. D. Tolley and M. L. Lee, *J. Sep. Sci.*, 2013, **36**, 2767-2781.

18. C. Yu, M. H. Davey, F. Svec and J. M. J. Fréchet, *Anal. Chem.*, 2001, **73**, 5088-5096.

19. J. D. Ramsey and G. E. Collins, *Anal. Chem.*, 2005, **77**, 6664-6670.

20. R. S. Foote, J. Khandurina, S. C. Jacobson and J. M. Ramsey, *Anal. Chem.*, 2005, **77**, 57-63.

21. Z. Long, Z. Shen, D. Wu, J. Qin and B. Lin, *Lab Chip*, 2007, **7**, 1819-1824.

22. Q. S. Kang, Y. Li, J. Q. Xu, L. J. Su, Y. T. Li and W. H. Huang, *Electrophoresis*, 2010, **31**, 3028-3034.

23. G. V. Kaigala, V. N. Hoang, A. Stickel, J. Lauzon, D. Manage, L. M. Pilarski and C. J. Backhouse, *Analyst*, 2008, **133**, 331-338.

24. B. H. Weigl, R. L. Bardell and C. R. Cabrera, *Adv. Drug Deliver. Rev.*, 2003, **55**, 349-377.

25. L. Zhang, X. Yin and Z. Fang, *Lab Chip*, 2006, **6**, 258-264.

26. G. S. Fiorini and D. T. Chiu, *Biotechniques*, 2005, **38**, 429-446.

27. V. Sahore, S. Kumar, C. I. Rogers, J. Jensen, M. Sonker and A. T. Woolley, *Anal. Bioanal. Chem.*, 2016, **408**, 599-607.

28. R. Yang, J. V. Pagaduan, M. Yu and A. T. Woolley, *Anal. Bioanal. Chem.*, 2015, **407**, 737-747.

29. M. A. Unger, H.-P. Chou, T. Thorsen, A. Scherer and S. R. Quake, *Science*, 2000, **288**, 113-116.

30. W. Yang, M. Yu, X. Sun and A. T. Woolley, *Lab Chip*, 2010, **10**, 2527-2533.

Table 1. Three- and five-valve peristaltic pump solution flow rates at different actuation frequencies.

Pump and solution	10 Hz operation	20 Hz operation
Three-valve		
ACN	*	120 nL/min
50% ACN + 50% Buffer	*	60 nL/min
30% ACN + 70% Buffer	*	40 nL/min
Buffer	*	30 nL/min
Five-valve		
90% ACN + 10% buffer	140 nL/min	330 nL/min
50% ACN + 50% Buffer	140 nL/min	280 nL/min
30% ACN + 70% Buffer	140 nL/min	210 nL/min
Buffer	140 nL/min	160 nL/min

* Solution flow at 10 Hz actuation for the three-valve pump was not measured because flow was very slow at 20 Hz operation. Each value given is the average of two measurements done in the same device.

FIGURE CAPTIONS

Figure 1. Design and fabrication of integrated SPE and μCE system. (A) Device schematic, 1: loading, 2: waste, 3: ground, and 4: high voltage reservoirs. (B) Control layer fabrication. (C) Fluidic layer fabrication. (D) Hot embossing of COC layer. (E) Schematic showing assembly of an integrated device. (F) A photograph of completed microchip; scale bar is 3 mm.

Figure 2. SPE and μCE integrated device with on-chip pneumatic valve structures. (A) Open valve configuration schematic showing vertical cross-section. (B) Closed valve configuration schematic. (C) Five-valve peristaltic pump in the SPE module with open valves. (D) Actuated valves. (E) Open pneumatic valve arrangement surrounding the intersection in the separation module. (F) Actuated valves. (G) Integrated device on a microscope stage with dye-filled control channels connected to external tubing.

Figure 3. Background-subtracted fluorescence of FITC-Fer on a C8 monolith under conditions for retention and elution.

Figure 4. Fer retention and elution on a C8 monolith. (A) C8 monolith CCD image of fluorescence before loading FITC-Fer; scale bar is 100 μm. (B) C8 monolith CCD image after loading FITC-Fer (700 nL) at 10 Hz and ~30 psi applied pressure for 5 min. (C) C8 monolith CCD image after a 90% ACN rinse using a five-valve pump. (D) Plots showing PMT detection (at the injection intersection) of FITC-Fer eluted in 90% ACN from the C8 monolith. Fer retention and elution were performed using (red) three- and (blue) five-valve peristaltic pumps, respectively. Loaded Fer concentrations were 100 nM (3-valve pump) and 200 nM (5-valve pump). A 10-point boxcar average was used to smooth the PMT data. The solution flow direction in (A-C) is from right to left.

Figure 5. Fluorescent data from a C8 monolith under different conditions of FITC-Fer retention or elution. (A) Buffer rinse; scale bar is 100 μm. (B) Fer loading for 2 min. (C) Fer loading for 5 min. (D) Fer loading for 10 min. (E) Rinse with 90% ACN. (F) Final rinse with 100% ACN. (G) Plot showing fluorescent intensity on a C8 monolith with different loading times and after elution. Solution flow in (A-F) is from right to left.

Figure 6. Microchip electropherograms showing the effects of on-chip sample enrichment. (A) Electrophoretic separation of FITC-Fer (100 nM) with enrichment on a C8 monolith and (B) without enrichment. (C) Electrophoretic separation of a mixture of two labeled peptides, FA and GGYR (both 500 nM), with enrichment on a C8 monolith and (D) without enrichment. The y-axis range in (A) is 10X greater than in (B-D).

Graphical abstract. Integrated microfluidic devices with pumps, valves, and a solid-phase extraction monolith provide improved signal in microchip electrophoresis.

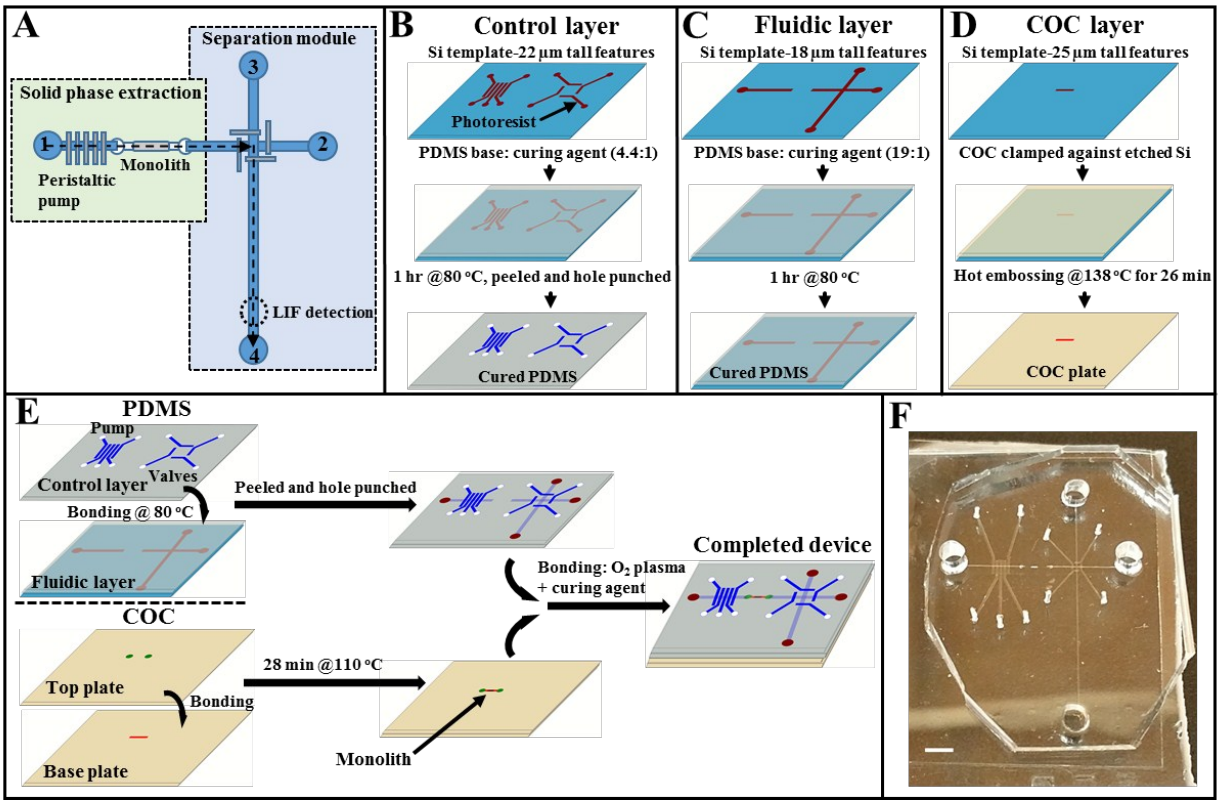

Figure 1. Design and fabrication of integrated SPE and µCE system. (A) Device schematic, 1: loading, 2: waste, 3: ground, and 4: high voltage reservoirs. (B) Control layer fabrication. (C) Fluidic layer fabrication. (D) Hot embossing of COC layer. (E) Schematic showing assembly of an integrated device. (F) A photograph of completed microchip; scale bar is 3 mm.

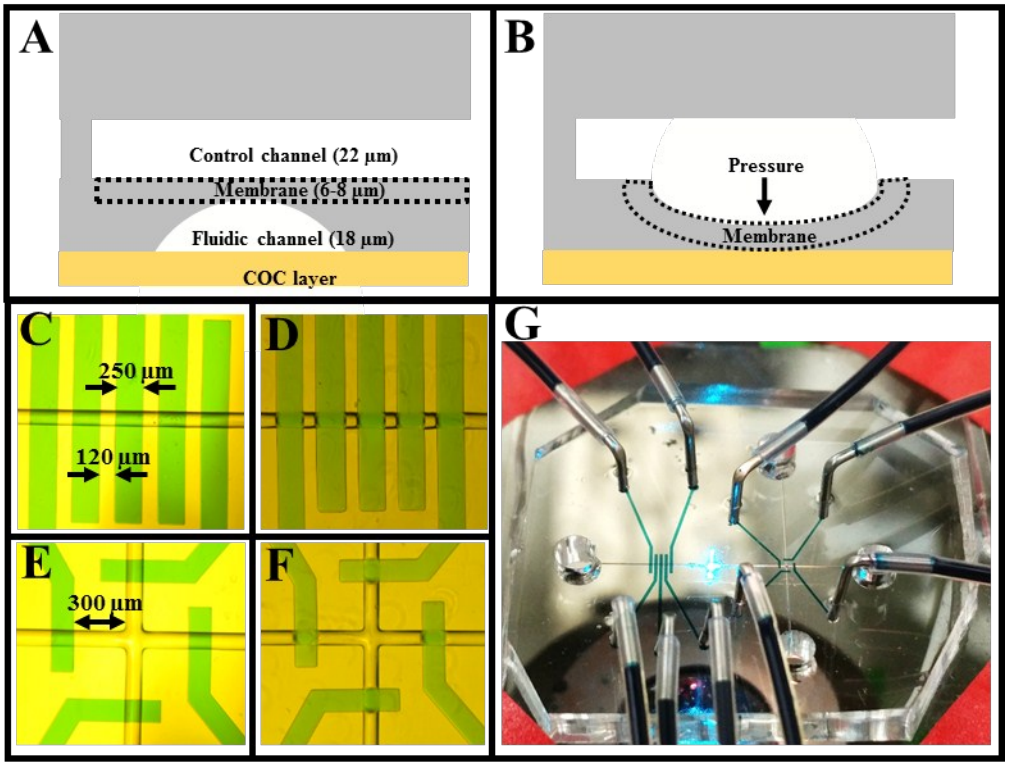

Figure 2. SPE and µCE integrated device with on-chip pneumatic valve structures. (A) Open valve configuration schematic showing vertical cross-section. (B) Closed valve configuration schematic. (C) Five-valve peristaltic pump in the SPE module with open valves. (D) Actuated valves. (E) Open pneumatic valve arrangement surrounding the intersection in the separation module. (F) Actuated valves. (G) Integrated device on a microscope stage with dye-filled control channels connected to external tubing.

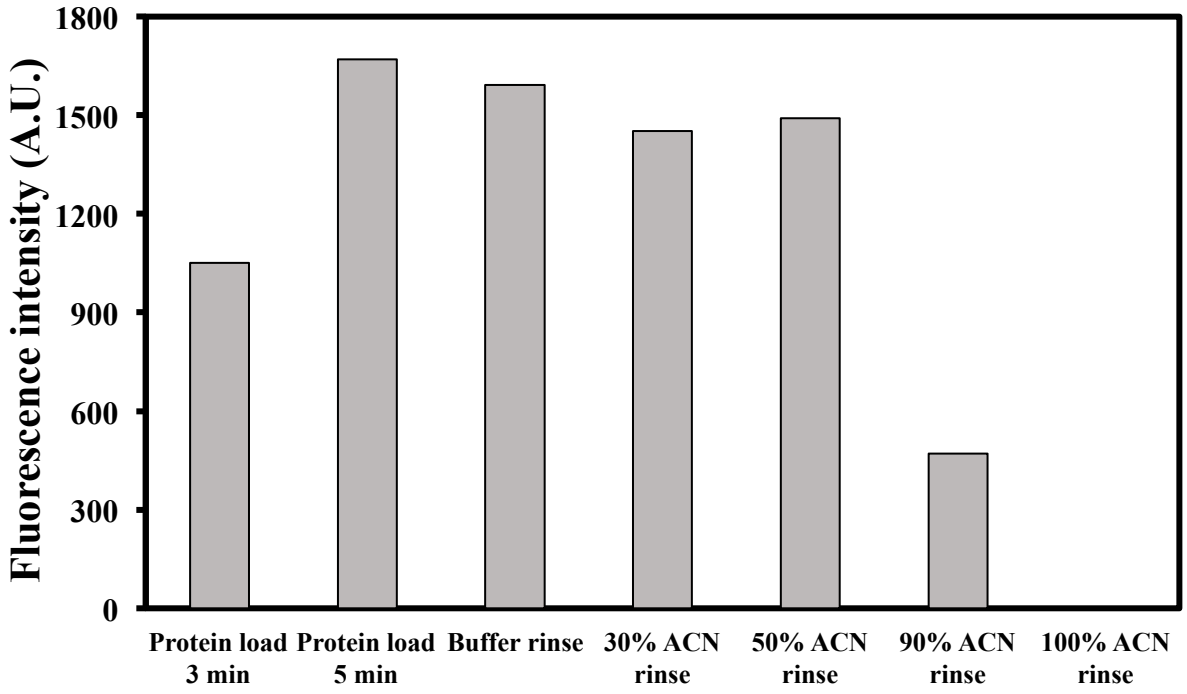

Figure 3. Background-subtracted fluorescence of FITC-Fer on a C8 monolith under conditions for retention and elution.

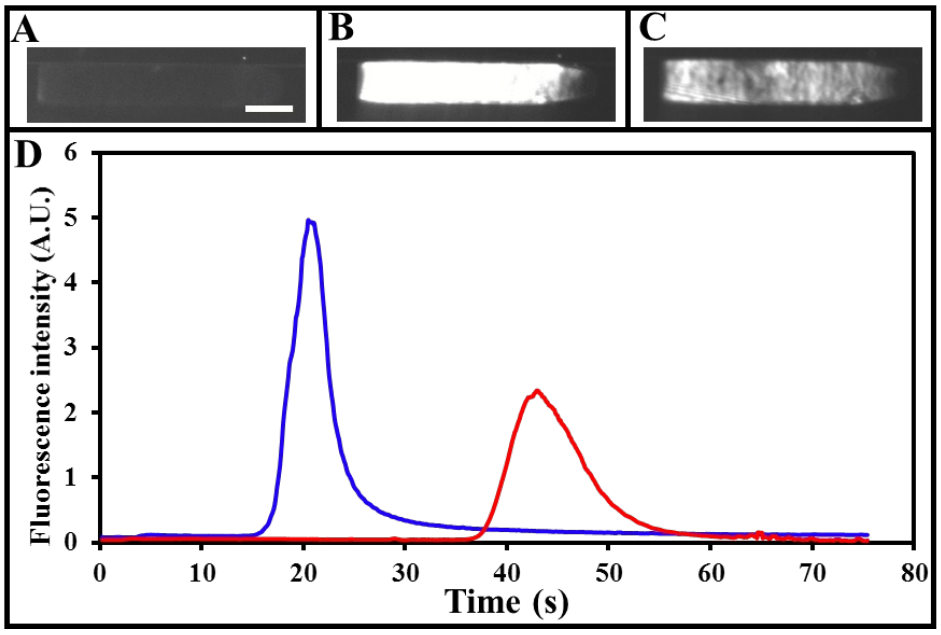

Figure 4. Fer retention and elution on a C8 monolith. (A) C8 monolith CCD image of fluorescence before loading FITC-Fer; scale bar is 100 µm. (B) C8 monolith CCD image after loading FITC-Fer (700 nL) at 10 Hz and ~30 psi applied pressure for 5 min. (C) C8 monolith CCD image after a 90% ACN rinse using a five-valve pump. (D) Plots showing PMT detection (at the injection intersection) of FITC-Fer eluted in 90% ACN from the C8 monolith. Fer retention and elution were performed using (red) three- and (blue) five-valve peristaltic pumps, respectively. Loaded Fer concentrations were 100 nM (3-valve pump) and 200 nM (5-valve pump). A 10-point boxcar average was used to smooth the PMT data. The solution flow direction in (A-C) is from right to left.

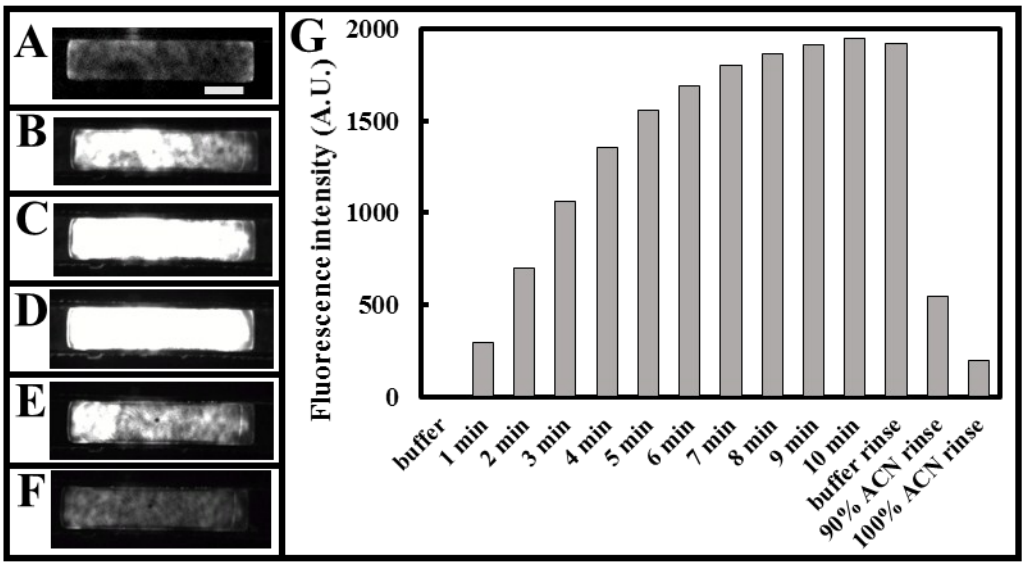

Figure 5. Fluorescent data from a C8 monolith under different conditions of FITC-Fer retention or elution. (A) Buffer rinse; scale bar is 100 μm. (B) Fer loading for 2 min. (C) Fer loading for 5 min. (D) Fer loading for 10 min. (E) Rinse with 90% ACN. (F) Final rinse with 100% ACN. (G) Plot showing fluorescent intensity on a C8 monolith with different loading times and after elution. Solution flow in (A-F) is from right to left.

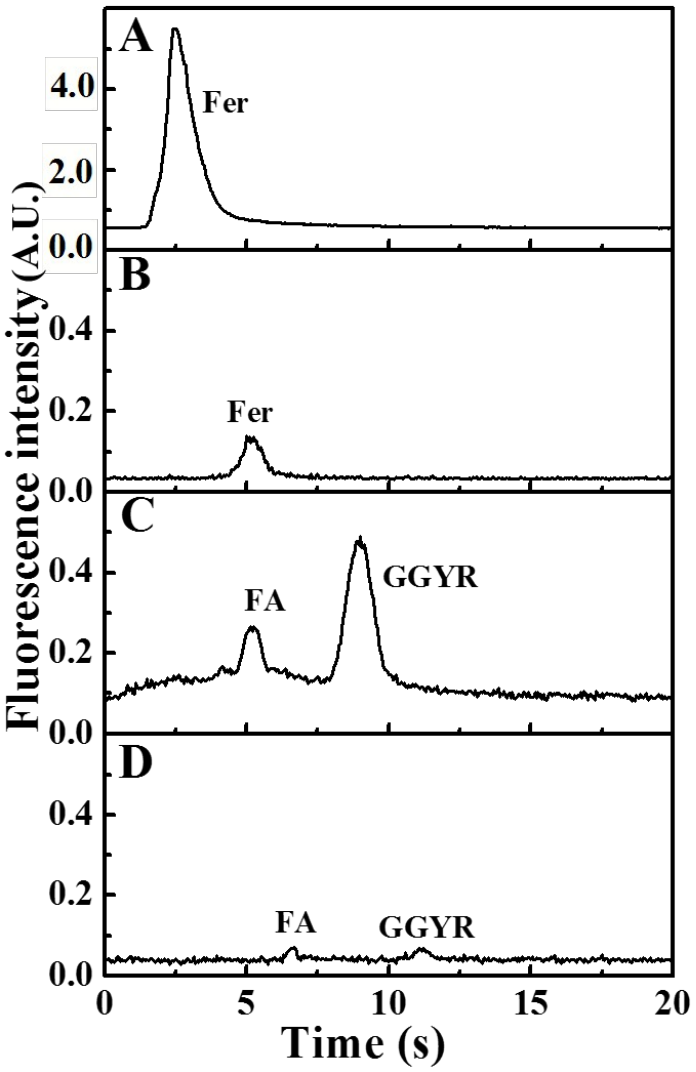

Figure 6. Microchip electropherograms showing the effects of on-chip sample enrichment. (A) Electrophoretic separation of FITC-Fer (100 nM) with enrichment on a C8 monolith and (B) without enrichment. (C) Electrophoretic separation of a mixture of two labeled peptides, FA and GGYR (both 500 nM), with enrichment on a C8 monolith and (D) without enrichment. The y-axis range in (A) is 10X greater than in (B-D).

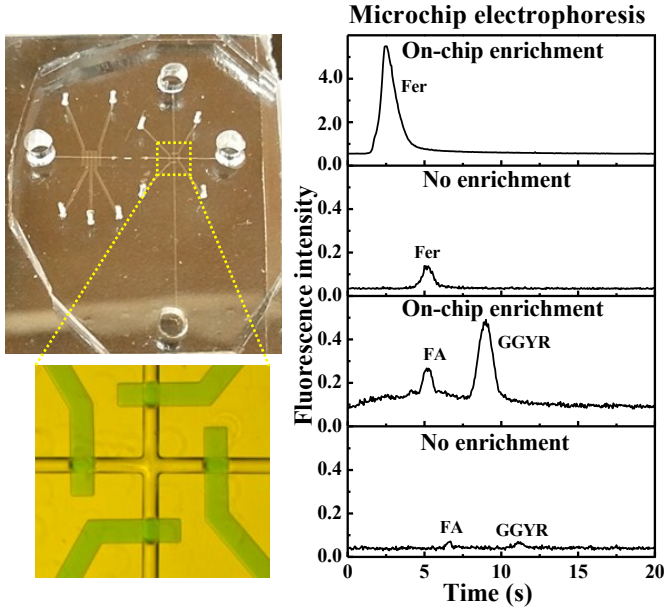

Graphical abstract. Integrated microfluidic devices with pumps, valves, and a solid-phase extraction monolith provide improved signal in microchip electrophoresis.